

## Signal Transmission in the Auditory System

### Academic and Research Staff

Professor Dennis M. Freeman, Professor William T. Peake, Professor Thomas F. Weiss, Dr. Alexander J. Aranyosi, Dr. Bertrand Delgutte, Dr. Donald K. Eddington, Aleem Siddiqui

### Visiting Scientists and Research Affiliates

Dr. H. Steven Colburn, Dr. John J. Rosowski, Michael E. Ravicz

### Graduate Students

Leonardo Cedolin, Salil Desai, Anne A. Dreyer, Roozbeh Ghaffari, Jianwen Wendy Gu, Kenneth E. Hancock, Courtney C. Lane, Kinuko Masaki, Hui Nam, Becky B. Poon, Chandran V. Seshagiri, Zachary M. Smith, Jocelyn Songer

### Technical and Support Staff

Janice Balzer

## 1. Middle and External

### Sponsor

National Institutes of Health (through the Massachusetts Eye and Ear Infirmary)  
Grants R01 DC00194, R01 DC04798

### Project Staff

Professor William T. Peake, Dr. John J. Rosowski, Michael E. Ravicz

The external and middle ears are important to auditory function as they are the gateway through which sound energy reaches the inner ear. Also, middle-ear disease is the most common cause of hearing loss, and while a wide range of treatments have been developed, many lead to unsatisfactory hearing results. We use measurements of middle-ear structure and function in animals, live human patients and cadaver ears in order to investigate the effects of natural and pathological variations of middle-ear structure on ear performance.

### 1.1 Comparative Structure and Function in Middle Ears

A review comparing middle-ear function in many animals and describing the extreme sensitivity of the auditory system to mechanical disturbances was published. The review described large differences in the frequency selectivity of the middle ear of different species that are related to the size and ossicular structure of these ears. However, at their best frequency, each of the ears can respond to tympanic-membrane displacements that are smaller than the diameter of a hydrogen atom.

### 1.2 The Effect of Ageing on Middle-Ear Function in Mouse

It has been suggested that age-related changes in the middle ear are at least partially responsible for the decreases in hearing sensitivity observed in aged humans and other animals. Our group addressed this issue, by quantifying middle-ear function in mice of different ages. The results describe small, but significant, decreases in middle-ear response with age accompanied by larger decreases in overall hearing sensitivity (Figure 1). We conclude that while age-related decreases in middle-ear function do occur, these decreases are small compared to the age-related decrease in the sensitivity of the total peripheral auditory system; therefore, age-related hearing loss is primarily an inner ear problem.

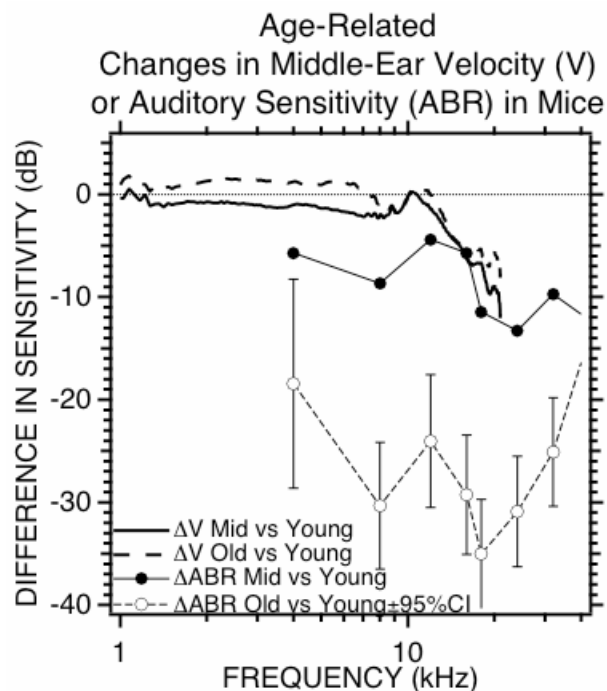


**Figure 1.** Changes in sensitivity of the middle ear  $\Delta V$  and the sensitivity of the animal to sound  $\Delta ABR$  (the auditory brainstem response) with age in one strain of mice, the SvEv129S6. The solid lines and the filled circles illustrate the measured changes between 6-8 week old mice and 12 month olds. The dashed lines and the open circles show changes between 6-8 weeks and 18-24 months. The N of each group is about 10. The vertical bars are 95% confidence intervals around the mean value. The change observed in ABR are significantly larger than the changes in velocity.

### 1.3 Measures of Middle-Ear Function in Human Ears with No Middle-Ear Pathology

A detailed description of the sound-induced velocity of the tympanic membrane in over 100 live human subjects with no middle-ear pathology was published. The measurements were made in awake subjects using a laser-Doppler vibrometer. The results define the normal range in our pathological studies. The measurements were made on subjects of ages from 20 to 80 years old, about half with normal hearing and half with measurable sensory-neural hearing loss. A significant linear relationship between sound-induced tympanic-membrane velocity and age was seen only at 6000 Hz (Figure 2A); however, this slope was much less steep than the slope between Auditory thresholds and age at a similar frequency (Figure 2B). No relationship was found between hearing thresholds and middle-ear velocity. This study and our previous work suggest that laser-Doppler vibrometry is a sensitive measure of sound-conduction function but is generally insensitive to sensory pathologies of the inner ear.

### 1.4 Measures of Middle-Ear Function in Diseased Middle Ears

We have used a human cadaver temporal-bone preparation and a retrospective analysis of the results of surgery to investigate reasons for 50% failure rate in reconstructive surgery for the loss of the tympanic membrane, malleus and incus (a so-called Type III tympanoplasty). These studies have identified two of the major causes of tympanoplastic failure as fixations of the remaining ossicle and failure of the middle-ear to aerate after surgery. However, hearing results appear less than optimal even in cases with aerated middle ears and mobile ossicles. A possible technical improvement, supported by the temporal-bone measurements, is to stiffen the graft tympanic membrane material so that the graft moves more uniformly. Preliminary surgical results with grafts stiffened by a thin cartilage sheet show a significant improvement in hearing result.

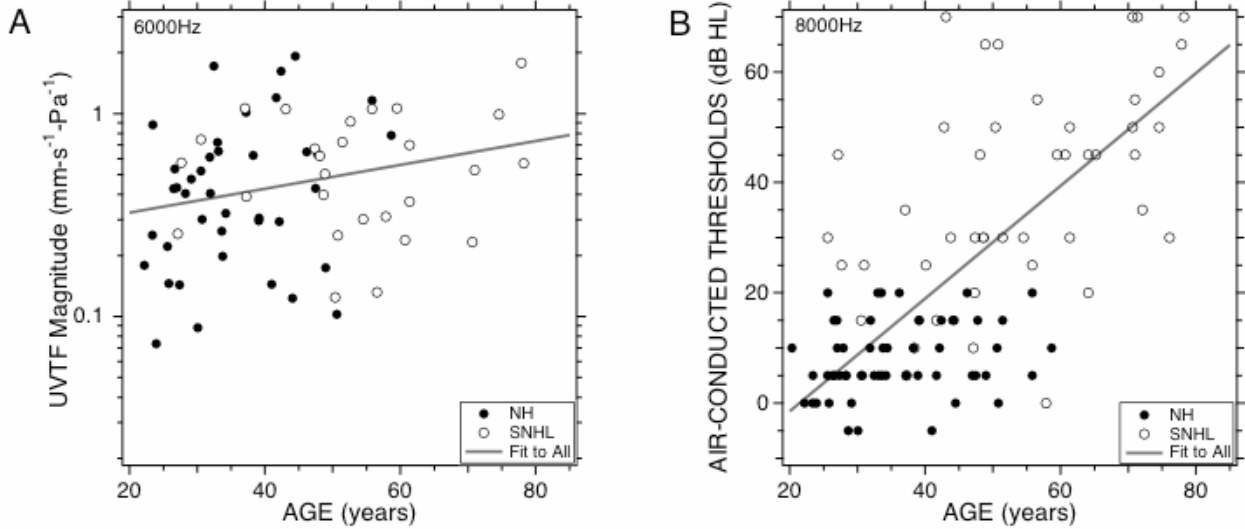


**Figure 2.** Measures of tympanic-membrane velocity and hearing thresholds in 101 human ears from subjects of varied ages. Results from normal hearing ears (filled circles) and ears with sensorineural hearing loss (open circles) are plotted. The lines are the results of a least-squares regression analysis, both of which are significant at the 5% level. (A) Magnitude of sound-induced tympanic membrane velocity normalized by ear-canal sound pressure (UVTF). (B) Hearing thresholds in dB HL.

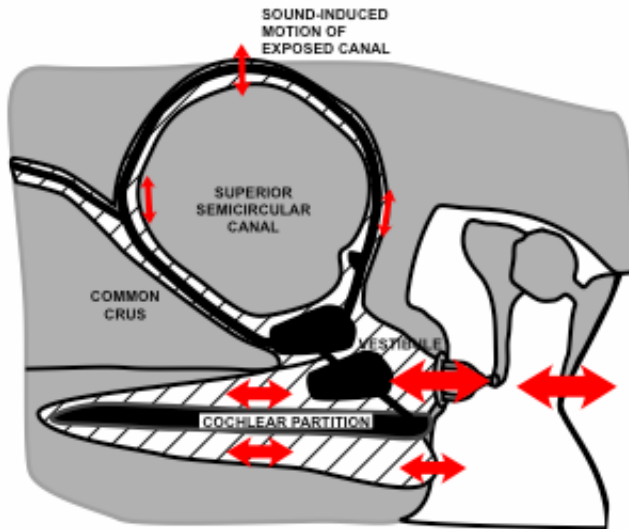


**Figure 3.** A model of the flow of sound through the inner ear in a patient with a superior semicircular dehiscence. In SSCD, some fraction of the volume-velocity into the inner ear is shunted away from the cochlear partition via the expose canal.

### 1.5 Measures of the Effect of a Vestibular Dehiscence on Auditory Function

A newly described clinical entity produced by a hole (a dehiscence) in the superior semicircular canal wall has been investigated by our group. While this pathology can produce a distinctive vestibular symptomatology, we have conducted a clinical study that documents a conductive hearing loss in a significant fraction of patients with this pathology. The hearing loss hypothetically results from a shunting of sound through the dehiscence and away from the auditory inner ear (Figure 3). We have also published some preliminary data that is consistent with this model: (a) We have demonstrated the existence of sound-induced motion of the vestibular lymph within a dehiscence in an animal model. (b) We have determined that patients with dehiscences have reduced cochlear input impedance.

### 1.6 Characterization of the Vibratory Characteristics of a Potential Material for Artificial Vocal Folds

Vocal fold vibration depends on the material properties of the mucosa that surrounds the fold. As yet, there is no adequate replacement for the natural mucosal, so that attempts to improve voice quality by replacing scarred folds have not been satisfactory. We have used our expertise in the generation and measurement of acousto-vibratory stimuli and responses to investigate the mechanical properties of a hydrogel developed by the Langer group in The Department of Chemical Engineering and the Mosher Laryngological Research Laboratory at the Massachusetts Eye and Ear Infirmary. These analyses have demonstrated that hydrogels can have resonance properties similar to those of the vocal folds and that these properties can be adjusted by variations in the chemical composition and hydration of the gel.

## Publications

### Journal Articles Published

R.H. Mehta, M.E. Ravicz, J.J. Rosowski, and S.N. Merchant, "Middle-ear Mechanics of Type III Tympanoplasty (Stapes Columella): I. Experimental Studies," *Otology and Neurotology*, 24:176-185 (2003).

S.N. Merchant, M.J. McKenna, R.H. Mehta, M.E. Ravicz, and J.J. Rosowski, "Middle-ear Mechanics of Type III Tympanoplasty (Stapes Columella): II. Clinical Studies," *Otology and Neurotology*, 24:186-194 (2003).

J.J. Rosowski, R.H. Mehta, and S.N. Merchant, "Diagnostic Utility of Laser-Doppler Vibrometry in Conductive Hearing Loss with Normal Tympanic Membranes," *Otology and Neurotology*, 24:165-175 (2003).

J.J. Rosowski, K.M. Brinsko, B.L. Tempel, and S.G. Kujawa, "The Ageing of the Middle Ear in 129S6/SvEvTac and CBA/CAJ Mice: Measurements of Umbo Velocity, Hearing Function and the Incidence of Pathology," *JARO*, 4: 371-383 (2003).

K.R. Whittemore, S.N. Merchant, B.B. Poon, and J.J. Rosowski, "A Normative Study of Tympanic-membrane Motion in Humans Using a Laser-Doppler Vibrometer," *Hear. Res.* 187: 85-104 (2004).

A.A. Mikulec, M.J. McKenna, M.J. Ramsey, J.J. Rosowski, B.S. Herrmann, S.D. Rauch, H.D. Curtin, and S.N. Merchant, "Superior Semicircular Canal Dehiscence Presenting as Conductive Hearing Loss without Vertigo," *Otology & Neurotology*, 25:121-129 (2004).

**Journal Articles Accepted for Publication**

J.J. Rosowski, J.E. Songer, H.H. Nakajima, K.M. Brinsko, and S.N. Merchant, "Investigations of the Effect of Superior Semicircular Canal Dehiscence on Hearing Mechanisms," *Otology & Neurotology*, forthcoming.

X. Jia, J.A. Burdick, J.B. Kobler, R.J. Clifton, J.J. Rosowski, S.M. Zeitels and R. Langer, "Synthesis and Characterization of *insitu* Crosslinkable Hyaluronic Acid-based Hydrogels with Potential Application for Vocal Fold Regeneration," *Macromolecules*, forthcoming.

**Books/ Chapters in Books**

J.J. Rosowski, "The Middle and External Ears of Terrestrial Vertebrates as Mechanical and Acoustic Transducers," in *Sensors and Sensing in Biology and Engineering*, eds. F.G. Barth, J.A.C. Humphrey, and T.W. Secomb, (New York: Springer-Verlag, 2003) pg. 59-69.

## 2. Cochlear Mechanics

### Sponsor

National Institutes of Health  
Grant R01 DC00238

### Project Staff

Professor Dennis M. Freeman, Professor Thomas F. Weiss, Dr. Alexander J. Aranyosi, Roozbeh Ghaffari, Kinuko Masaki

## 2.1. Material Properties of the Tectorial Membrane

### Introduction

The tectorial membrane (TM) is a gelatinous structure that lies on top of the mechanically sensitive hair bundles of sensory cells in the inner ear. From its position alone, we know that the TM must play a key role in transforming sounds into the deflections of hair bundles. But the mechanisms are not clear, largely because the TM has proved to be a difficult target of study. It is 97% water, and is therefore fragile. It is small: the whole TM would roll up and fit into little more than an inch of one human hair. Finally, it is transparent.

We have developed methods to isolate the TM so that its properties can be studied. Results using this technique (reported in previous RLE Progress Reports) show that the TM behaves as a gel. The material properties of a gel are a direct consequence of its molecular architecture. Charge groups on gel macromolecules attract mobile counterions from the surrounding fluid. Thus gels concentrate ions, and thereby increase osmotic pressure. The increase in osmotic pressure induces water to move into the gel and cause it to swell. The swelling stretches the macromolecules and increases the stiffness of the gel. The important consequence is that gels have mechanical, electrical, osmotic, and chemical behaviors that are all linked by their common molecular basis.

### Measuring Electromechanical Motions of the TM

The presence of charged molecules fixed to the TM macromolecules<sup>1</sup> suggests an analogy with cartilage in which electrical and mechanical properties are inextricably coupled<sup>2</sup>. However, experiments to measure TM electrical properties have proven to be difficult. Steel<sup>3</sup> provided the first direct measurements of TM electrical potential but found it was difficult to get stable and repeatable recordings. Indirect measurements based on volume change<sup>4, 5</sup> were more stable but difficult to interpret.

---

<sup>1</sup> I. Thalmann, K. Machiki, A. Calabro, V.C. Hascall, and R. Thalmann, "Uronic Acid-containing Glycosaminoglycans and Keratan Sulfate are Present in the Tectorial Membrane of the Inner Ear: Functional Implications," *Arch. Biochem. Biophys.*, 307: 391-396 (1993).

<sup>2</sup> S.R. Eisenberg and A.J. Grodzinsky, "Swelling of Articular Cartilage and Other Connective Tissues: Electromechanochemical Forces," *J. Orthopaedic Res.*, 3: 148-159 (1985).

<sup>3</sup> K.P. Steel, "The Tectorial Membrane in Mammals," *Hearing Res.*, 9: 327-359 (1983).

<sup>4</sup> A. Kronester-Frei, "The Effect of Changes in Endolymphatic Ion Concentrations of the Tectorial Membrane," *Hearing Res.*, 1:81-94 (1979).

<sup>5</sup> D.M. Freeman, S.M. Hattangadi, and T.F. Weiss, "Osmotic Responses of the Isolated Mouse Tectorial Membrane to Changes in pH," *Auditory Neurosci.*, 3: 363-375 (1997).

To develop a stable and direct method of probing TM electrical properties, we created microfabricated experiment chambers containing gold patterned electrodes. TM preparations were isolated from mice and placed across gold electrodes as the TM was bathed in artificial endolymph. AC voltage stimuli (800 mV peak, 1 kHz) were applied to the electrodes to stimulate the TM. Electrically evoked TM displacements were measured using two independent techniques – laser interferometry and atomic force sensing<sup>6</sup>.

We observed motion of the surface of the TM in response to voltage stimuli. The electromotile response of the TM had an average peak amplitude of 1–4 nm (Figure 1). To ensure that this motion was not due to mechanical vibration of the electrodes, we repeated measurements on the surface of the electrodes. The peak amplitude of motion for these control measurements was approximately 0.02 nm, much smaller than the observed TM motion. The electromotile response was also pH dependent – when the bathing solution had a pH < 4, the phase of electrically-induced motion changed by 180° (Figure 2). This result is consistent with a previous study<sup>5</sup> showing that the fixed charge within the TM changes sign for low pH values, providing additional evidence that the electromotile response seen in this study depends on the presence of fixed charges within the TM.

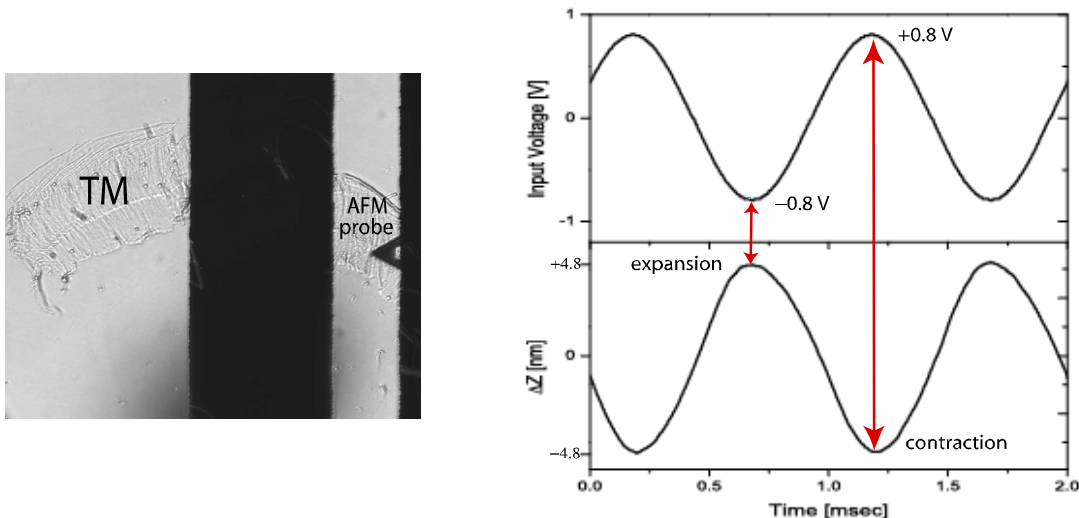


**Figure 1.** (Left) Light microscope image showing the AFM tip engaged on the surface of the TM sample. (Right) Input voltage and resulting TM motion as a function of time. TM displacement is about 180° out of phase with the input voltage, indicating that the TM's surface expands in response to negative voltage and contracts in response to positive voltage.

We interpret the observed motion as resulting from a force exerted on the fixed charge by the applied electric field. This force then acts on the stiffness of the collagen matrix to cause the motion. Such coupling of mechanical and electrical properties is inconsistent with traditional lumped-element models of the TM, but consistent with the predictions of a gel model of the TM<sup>7</sup>, and is analogous to the electromechanical properties of cartilage.

<sup>6</sup> I. Rousso, E. Kachatryan, Y. Gat, I. Brodsky, M. Ottolenghi, M. Sheves, and A. Lewis, "Microsecond Atomic Force Sensing of Protein Conformational Dynamics: Implications for the Primary Light-induced Events of Bacteriorhodopsin" *Proc. Nat'l. Acad. Sci.*, pp. 7937-7941 (1997).

<sup>7</sup> T.F. Weiss and D.M. Freeman, "Equilibrium Behavior of an Isotropic Polyelectrolyte Gel Model of the Tectorial Membrane: The Role of Fixed Charges, *Auditory Neurosci.*, 3: 351-361 (1997).

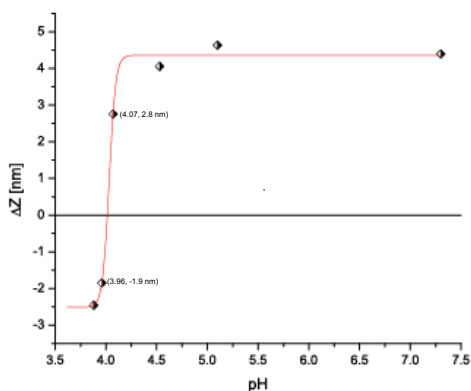


**Figure 2.** Changes in motion of the TM during perfusions of acidic solutions. The magnitude of TM motion decreased at low pH values. Below pH 4.07, we recorded a 180° shift in the motion of the TM. The  $pK_a$  of this transition was near 4.

### Measuring the Equilibrium Stress-Strain Relation of the TM

We have previously developed a technique for measuring the stress/strain relation of the TM using solutions containing polyethylene glycol (PEG). PEG is available in many different molecular weights (MWs). PEG with large MW cannot penetrate the TM, and so exerts an osmotic force on the TM when it is reflected off of the surface. PEG with small MW can penetrate the TM, causing little osmotic force. During the past year, we measured the osmotic response of the TM to PEG solutions to obtain information not only about the bulk modulus, but about the molecular architecture of the TM, such as its pore size. Pore size was determined by measuring the osmotic response of the TM to PEG solutions with the same osmotic pressure, but differing MW. We found that PEG with a MW greater than 200 kDa systematically generated greater osmotic response than PEG of smaller MW, implying that PEG with lower MWs may have entered the TM. These results suggest that the effective pore size of the TM is on the order of 10 nm, indicating that proteins smaller than about 200 kDa may be able to diffuse through the TM.

The stress/strain relation of the TM was determined by measuring the osmotic response of the TM to varying concentrations of PEG with MW greater than 200 kDa. At low PEG concentrations, the osmotic response was proportional to the osmotic pressure (Figure 3). From this relation, the bulk modulus was determined to be on the order of 0.9 kPa. This number is smaller than previous estimates which were made using PEG with a MW of 20 kDa. The difference is likely to be due to the smaller PEG entering the TM, and thus exerting a lower osmotic pressure than expected. At higher osmotic pressures the TM exhibited significant strain hardening. This effect is most likely caused by electrostatic repulsion of the fixed charges present within the TM. We are currently preparing a manuscript of these results for publication.

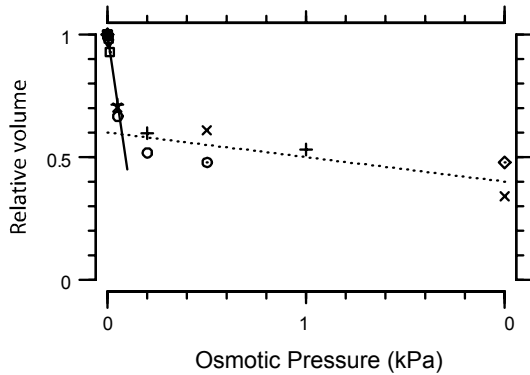


Figure 3. Relative volume of the TM as a function of applied osmotic pressure. At low osmotic pressures, the TM shrinks linearly with increasing osmotic pressure. The solid line has a slope of  $-(0.9 \text{ kPa})^{-1}$ . At higher osmotic pressures, the TM exhibits strain hardening. The dotted line has a slope of  $-(17 \text{ kPa})^{-1}$ .

### Characterizing TMs from COL11A2 $-/-$ Mice

The COL11A2 gene encodes the  $\alpha 2$  variant of collagen type XI, which is expressed in the TM. Mutations in this gene cause a 40–60 dB hearing loss in both humans and mice,<sup>8,9,10</sup> and cause disruptions of the fibrillar structure of the TM. To explore the mechanical consequences of the mutation, we have performed a series of measurements to study the material properties of TMs from COL11A2  $-/-$  and  $+/-$  mice. Although this characterization is incomplete (the COL11A2 mutants were genotyped after the TM measurements were performed, and the sample contained no wild-types), comparisons to TMs from wild-type mice of another strain show important differences. The overall appearance of TMs from COL11A2  $-/-$  mice in a light microscope was similar to that of TMs from wild-type mice. However, there were thickness differences: TMs from the homozygotes were thinner at a given longitudinal position than wild-types, while TMs from heterozygotes had a thickness comparable to wild-types.

The stress/strain relation of the TM was studied by applying solutions containing various concentrations of polyethylene glycol (PEG), as described in the previous section. We have found that TMs from homozygotes shrank by a smaller fraction than those from wild-type mice at a given PEG concentration. Consequently, at large osmotic pressures the absolute volumes of TMs from mutant and wild-type mice were similar. TMs from heterozygotes were similar to wild-types.

There are several possible mechanisms that could cause these differences. The TMs of homozygotes could have a larger bulk modulus. Alternately, the pores in homozygous TMs could be larger, allowing PEG of larger molecular weights to permeate and thereby increase the apparent stiffness of the TM. A third possibility is that the fixed charge concentration of TMs from homozygotes could be greater, adding apparent bulk modulus from electrostatic repulsion. The difference may also reflect a difference between the strains used for the knockout and the wild-type mice. Finally, the differences in bulk modulus could be a consequence of the differing thickness between homozygous and wild-type TMs. We are currently designing experiments to test these hypotheses.

<sup>8</sup> W.T. McGuirt, S.D. Prasad, A.J. Griffith, H.P. Kunst, G.E. Green, K.B. Shpargel, C. Runge, C. Huybrechts, R.F. Mueller, E. Lynch, M.C. King, H.G. Brunner, C.W. Cremers, M. Takanosu, S.W. Li, M. Arita, R. Mayne, D.J. Prockop, G. Van Camp, R.J. Smith, "Mutations in COL11A2 Cause Non-Syndromic Hearing Loss (DFNA13)", *Nat. Genet.*, 23(4): 413-9 (1999).

<sup>9</sup> E.M. De Leenheer, H.H. Kunst, W.T. McGuirt, S.D. Prasad, M.R. Brown, P.L. Huygen, R.J. Smith, and C.W. Cremers, "Autosomal Dominant Inherited Hearing Impairment Caused by a Missense Mutation in COL11A2 (DFNA13)", *Arch. Otolaryngol. Head Neck Surg.*, 127(1): 13-17 (2001).

<sup>10</sup> R.J. Ensink, P.L. Huygen, R.L. Snoeckx, G. Caethoven, G. Van Camp, and C.W. Cremers, "A Dutch Family with Progressive Autosomal Dominant Non-Syndromic Sensorineural Hearing Impairment Linked to DFNA13," *Clin. Otolaryngol.*, 26(4): 310-316 (2001).

## 2.2. Mechanical Properties of the Cochlea

### Sponsor

National Institutes of Health  
Grant R01 DC00238

### Project Staff

Professor Dennis M. Freeman, Professor Thomas F. Weiss, Dr. Alexander J. Aranyosi, Jianwen Wendy Gu

### Introduction

Many biological and man-made structures move in response to mechanical or electrical stimuli in the kHz-MHz frequency range. We have developed a system called Computer Microvision (CMV) to study the motions of such structures. The system consists of a microscope with a digital camera, a stimulus generator, and a light source that can be strobed at high frequencies. The structure under observation is placed on the microscope stage and driven with a periodic signal. The stimulus generator simultaneously drives the light source, an LED, with a pulse wave at the same frequency as the drive signal but with a small duty cycle. The camera is exposed for many cycles of the stimulus; the resulting image captures the position of the structure at the phase determined by the LED pulse. By taking images at several different phases, and repeating this process at successive planes of microscope focus, we capture the three-dimensional motion of the structure in response to the stimulus. Computer vision algorithms allow us to quantify the motion from the resulting images. CMV can sense motions as small as one nanometer, much smaller than the wavelength of light used to illuminate the specimen.

One important application of this technique is in the study of the cochlea, which is responsible for turning the mechanical vibrations of sound into neural signals. The mechanical properties of the cochlea are highly nonlinear and poorly understood. We have applied CMV to measure the motion of an entire cochlea in response to sound stimulation, and to study the material properties of one of the most enigmatic cochlear structures, the tectorial membrane (TM).

### Experimental Measurements of TM Dynamic Stiffness

The mechanical properties of the TM play a critical role in determining the response of the cochlea to sound stimulation. These mechanical properties have been difficult to measure, not only because of the micrometer size scale of the TM, but because of the nanometer-scale displacements at kilohertz frequencies induced by sound stimulation. We have developed a novel microfabricated force probe to overcome these difficulties.

The force probe consists of a microfabricated plate, 30  $\mu\text{m}$  on a side, connected to a stable base by a pair of cantilevered springs that form a diamond shape (Figure 4). The plate is placed on the TM, and piezoelectric crystals are used to impose sinusoidal displacements of the base in three dimensions. CMV is used to measure the resulting displacement of both the base and the plate. The difference in motion depends on the stiffness  $K_p$  of the probe arms and on the impedance of the TM seen by the plate. By calibrating  $K_p$  against an AFM probe of known stiffness, we can determine the impedance of the TM in three dimensions as a function of frequency and applied force. This method allows us to measure TM displacements at nanometer scales in response to sinusoidal forces with frequencies up to 10 kHz.

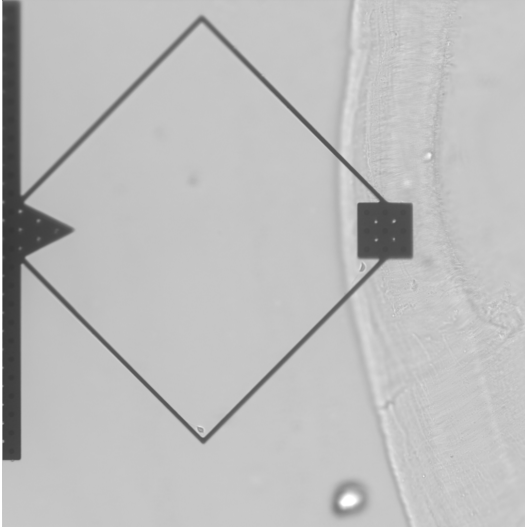


**Figure 4.** MEMS probe on TM sample. The probe consists of a base and shearing plate connected by two flexible arms. The 30x30  $\mu\text{m}$  shearing plate contacts a portion of the TM normally contacted by a 3x3 array of outer hair cells, which are mimicked by projections from the shearing plate. The probe is capable of applying forces in the radial, longitudinal and transverse directions. The fibrillar structure of the TM is readily visible in the image and was used to align the radial and longitudinal axes.

We have made preliminary measurements of motion in response to forces applied in both the radial and longitudinal directions for three TMs. TM displacement was linearly proportional to applied force for forces ranging from 0-100 nN. Forces in the longitudinal direction induced larger displacements than forces in the radial direction, indicating that the stiffness of the TM was roughly 60% larger in the radial direction.

The TM impedance contained both viscous and elastic components, with the elastic component being 4-5 times larger than the viscous component. This ratio was nearly constant with frequency. The impedance fell with frequency with a slope of about -0.8 for frequencies up to 10 kHz. These results suggest that the TM behaves as a distributed viscoelastic system (Figure 5).

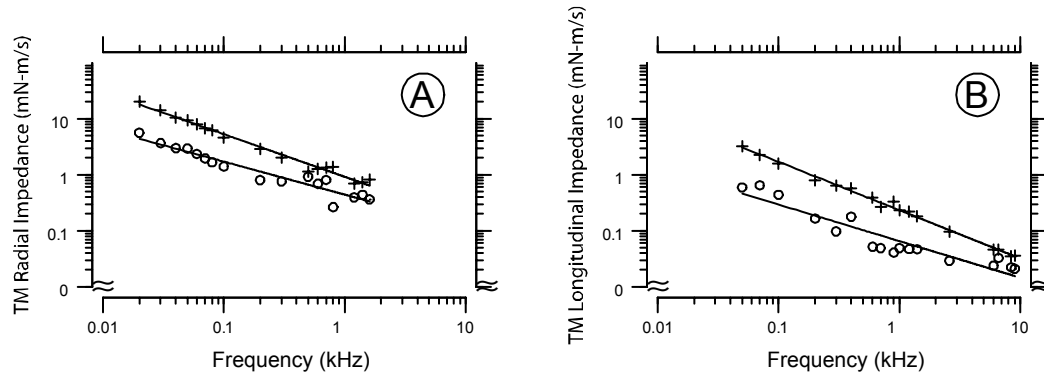


**Figure 5.** TM impedance versus frequency. Radial (A) and longitudinal (B) TM impedance vs. frequency for one TM. The elastic component of impedance (+) was typically 4-5 times larger than the viscous component (o) at all frequencies in both the radial and longitudinal directions. Radial impedance was about three times larger than longitudinal impedance. Least-squares fit lines have slopes of  $-0.8 \pm 0.14$  on a log-log scale.

### Sound-induced Motions of Cochlear Hair Bundles

Mechanical vibrations caused by sound are detected by hair cells in the cochlea. The organization of hair cells and supporting cells into a tissue determines the mechanical properties of the cochlea. To better understand the mechanics of hearing, we are studying the motions of the cochlea and its component structures in response to sound stimulation. To this end, our group has developed an in vitro preparation for studying cochlear mechanics. The cochlea of an alligator lizard is clamped in an experiment chamber so that it can be stimulated with sound while being imaged with the CMV system. Quantitative measurements of the relative motion of different structures within the cochlea help to improve our understanding of this critical stage in the hearing process.

During the past year, we have performed a detailed analysis of measurements of the dynamic mechanical behavior of hair bundles, the sub-cellular structures that confer mechanical sensitivity to the cochlea. Incoming sound causes motion of the bases of the hair bundles. The tips of the bundles, which are free-standing in this cochlea, move in response to fluid forces induced by motion of the cell bodies.

Our measurements revealed that although the magnitude of motion of the tips and bases of hair bundles was comparable at all frequencies measured, the relative phase was a strong function of frequency (Figure 6). At low frequencies, the tips and bases of hair bundles moved in phase with each other. At high frequencies, the tips increasingly lagged the bases; this lag approached  $-180^\circ$  at the highest frequencies. This phase lag was not well-fit by an ideal time delay. However, the lag was well fit by a model of hair bundle motion which takes the distributed mechanical properties of cochlear fluids into account<sup>11</sup>.

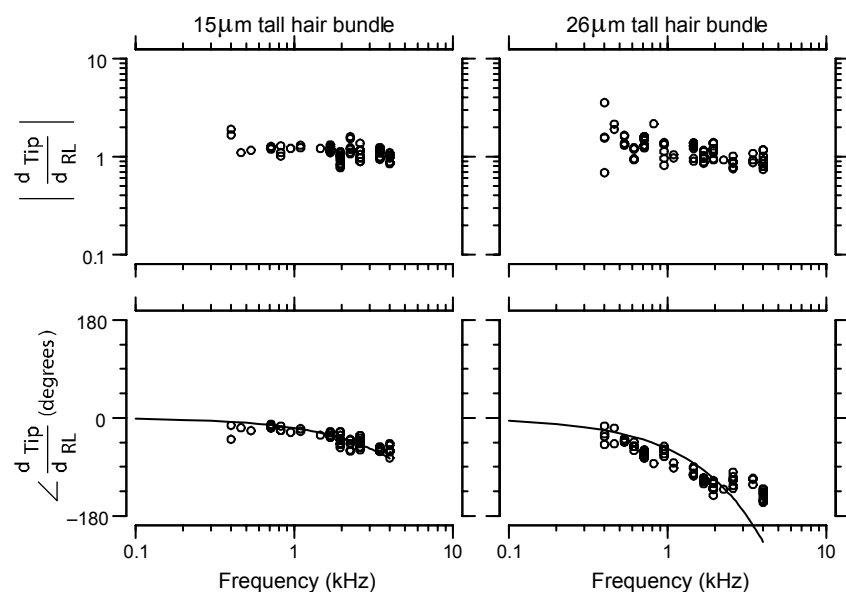


**Figure 6.** The magnitude (top) and phase (bottom) of the ratio  $d_{\text{Tip}}/d_{\text{RL}}$  of displacement of the tips and bases of individual hair bundles, for both a short (left) and tall (right) bundle. Although the magnitude was roughly constant with increasing frequency, the phase showed increasing lag. The solid lines in the phase plots are the least-squares fits of an ideal time delay to the phase measurements. The fit is reasonable for the shorter bundle, but for the taller bundle the ideal time delay underestimates the phase lag at lower frequencies and overestimates it at higher frequencies.

Hair bundle deflection is determined by subtracting displacement of the bundle tip from that of the base. At low frequencies, where the tip and base move in phase, hair bundle deflection is small and difficult to

<sup>11</sup> D.M. Freeman and T.F. Weiss, "Hydrodynamic Analysis of a Two-dimensional Model for Micromechanical Resonance of Free-standing Hair Bundles," *Hear. Res.*, 48:37-68 (1990).

measure. However, deflection magnitude increases with frequency, approaching a constant value at the highest frequencies. The phase of hair bundle deflection falls from above  $+90^\circ$  at low frequencies to near  $0^\circ$  at high frequencies. The dependence of hair bundle deflection on bundle height can be examined by measuring the frequency at which this phase lead falls below  $+60^\circ$  (Figure 7). This frequency is a strong function of bundle height, and is roughly comparable to the dependence of the hair cells' most sensitive frequency with bundle height. These results indicate that the mechanical interaction of hair bundles with the surrounding fluid is the primary determinant of frequency selectivity in this cochlea.

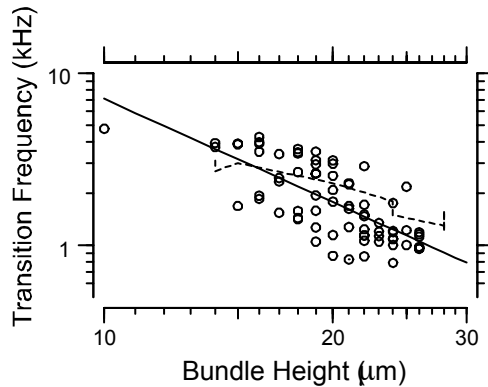


**Figure 7.** The frequency at which the phase of hair bundle deflection led the phase of displacement of the bundle base by  $+60^\circ$ . The solid line has a slope of  $-2.0$  on a log-log scale. The dashed line plots the best frequencies of hair cell receptor potentials as a function of bundle height.

#### Meeting Papers Published

A.J. Aranyosi, and D. M. Freeman, "Frequency Selectivity of Free-Standing Hair Bundles," podium presentation at *Twenty-Sixth Midwinter Research Meeting of the Assoc. for Research in Otolaryngology*, February 2003.

K. Masaki, R.J. Smith, and D.M. Freeman, "Comparing Material Properties of Tectorial Membranes From Normal and COL11A2  $-/-$  Deficient Mice," poster at *Twenty-Sixth Midwinter Research Meeting of the Assoc. for Research in Otolaryngology*, February 2003.

#### Journal Articles Published

D.M. Freeman, C.C. Abnet, W. Hemmert, B.S. Tsai, and T.F. Weiss, "Dynamic Material Properties of the Tectorial Membrane: A Summary," *Hearing Research* 180: 1-10, 2003.

D.M. Freeman, K. Masaki, A.R. McAllister, J.L. Wei, and T.F. Weiss, "Static Material Properties of the Tectorial Membrane: A Summary," *Hearing Research* 180: 11-27, 2003.

A.J. Aranyosi and D.M. Freeman, "Sound-induced Motions of Individual Cochlear Hair Bundles," *Biophys J*, submitted.

#### Undergraduate Projects

G. Chan, "Diagnostic Tests of Mice with Genetic Hearing Disorders," Advanced Undergraduate Project (AUP) in EECS, January 2004.

**Masters Theses**

R. Ghaffari, *Measuring Electrical Properties of the Tectorial Membrane*, M. Eng. in EECS, June 2003.

### 3. Neural Mechanisms for Auditory Perception

#### Sponsor

National Institutes of Health – National Institute on Deafness and Communication Disorders  
Grants DC02258 and DC00038

#### Project Staff

Dr, Bertrand Delgutte, Leonardo Cedolin, Kenneth E. Hancock, Courtney C. Lane, Chandran V. Seshagiri, Anne A. Dreyer

The long-term goal of our research is to understand the neural mechanisms that mediate the ability of normal-hearing people to process speech and other sounds of interest in the presence of competing sounds and how these mechanisms are degraded in the hearing-impaired. In the past year, we made progress in a number of research areas including the neural representation of pitch, neural mechanisms for binaural hearing, and studies of responses of local populations of neurons in the auditory midbrain.

#### 3.1 Neural Representations of Pitch in the Auditory Nerve

Previous neurophysiological studies have documented a robust representation of pitch in the interspike intervals of auditory-nerve (AN) fibers, but failed to find place cues to pitch, perhaps because they typically used stimuli with F0s in the range of human voice, for which harmonics are unlikely to be resolved in animals. We therefore investigated the representation of pitch in the AN for a much wider range of F0 than in previous studies, including the range of cat vocalizations.

We recorded responses of AN fibers in anesthetized cats to complex tones with a missing fundamental at moderate sound levels. The harmonics were of equal amplitude and in cosine phase. For most fibers, the average discharge rate was greater when the CF coincided with a low-order harmonic than when it fell between two harmonics. In general, harmonics up to about the 5th were thus resolved in rate responses at moderate stimulus levels. Using data from 20-50 AN fibers, we were able to estimate F0 with errors smaller than 2-3% by fitting a harmonic template to the rate-CF profiles. However, relatively few reliable estimates were obtained for F0 below 500 Hz, due to the broad cochlear tuning at low frequencies in the cat.

We also generated pooled interspike interval distributions by summing all-order interval histograms from all the sampled fibers. By fitting a periodic template to the pooled distributions, we were able to estimate F0 with errors smaller than 1-2% for frequencies up to 1300 Hz.

Our results suggest that both rate-place and interspike-interval representations of pitch are viable over a wide range of F0 in the cat, but the interval representation is more useful at lower F0s, and the rate-place representation at higher F0s. However, neither representation is entirely satisfactory in accounting for psychophysical data. The rate-place representation degrades with increasing sound level and fails to account for the upper frequency limit of musical pitch, while the interspike-interval representation does not account for the greater salience of pitch based on resolved harmonics compared to pitch based on unresolved harmonics. Future studies will investigate a spatio-temporal representation of pitch that seeks to combine the advantages and overcome the limitations of rate-place and interspike-intervals representations.

#### 3.2 Model of ITD Discrimination Based on Neural Responses in Auditory Midbrain

Understanding the neural coding of interaural time differences (ITD) is important because ITD is the main cue for localizing sounds containing low-frequency components, and differences in ITD contribute to the release from masking that occurs when a target sound source is spatially separated from a masker. ITD is represented in the inferior colliculus (IC) by cells that respond maximally at a particular best interaural delay (BD). In the conventional view of ITD coding, characteristic frequency (CF) and BD are distributed independently within the ITD processing mechanism to form a two-dimensional place map. However,

recent evidence from the guinea pig IC indicates that BD is actually inversely correlated with CF. We confirmed this finding for the cat IC, generalizing the observation across species and head sizes.

Previous studies have shown that single ITD-sensitive cells contain sufficient information in their average discharge rates to account for psychophysical ITD acuity on the midline. If ITD discrimination off the midline were based on the activity of the most sensitive cell available, then ITD acuity should be relatively constant over the physiological range of ITDs because cells with maximum acuity are found throughout this range. Contrary to this prediction, the ITD acuity of human listeners for broadband noise actually degrades as the base ITD moves away from the midline. To account for these results, we hypothesized that pooling of information across neurons may be essential for ITD discrimination, and tested this hypothesis by developing a neural model of ITD discrimination based on the response properties of ITD-sensitive cells in the IC of anesthetized cats.

We first developed a version of the binaural cross-correlator model that can be fit efficiently to single-unit rate-ITD curves. The model includes peripheral bandpass filters, an internal delay and phase shift, a crosscorrelator, and a quadratic function to convert interaural correlation into firing rate. The model parameters derived from the data were then used to constrain a population model of ITD discrimination. The population model accurately predicts ITD acuity as a function of ITD for broadband noise, but only if responses are first integrated (pooled) across CF.

Our results show that, even though single IC neurons may provide sufficient information to account for ITD acuity on the midline, pooling of information across neurons is needed to account for the degradation in acuity away from the midline. This pooling essentially implements a “straightness weighting” to emphasize ITDs that are consistent across CF. Thus, the auditory system seems to place a premium on the consistency of ITD information across frequency at the expense of ITD acuity on the periphery. This conclusion has implications for models of binaural processing that rely on analyzing ITD information within individual frequency channels.

### **3.3 Neural Correlates and Mechanisms of Spatial Release from Masking**

Normal-hearing listeners have a remarkable ability to hear in noisy environments, while hearing-impaired listeners and automatic speech-recognition systems often have difficulty in noise. We studied the neural mechanisms involved in one aspect of listening in noise, spatial release from masking (SRM), the improvement in detectability when a signal source is spatially separated from a masking source. We used neurophysiology, modeling, and psychoacoustics to investigate the neural mechanisms of SRM, focusing on low frequencies, which are important for speech recognition and are often spared in hearing-impaired listeners. At low frequencies, listeners use differences in ITD to improve signal detection when the signal and masker differ in azimuth. Unlike previous neurophysiological studies of the binaural detection of pure tone signals in noise, we used broadband signals more representative of natural sounds.

We recorded the responses of low-frequency, ITD-sensitive units in the IC of anesthetized cats for a broadband signal (a chirp train with a 40-Hz repetition rate) in continuous broadband noise. At low noise levels, neural discharges phase locked to the chirp train. As the noise level increased, the signal response was either overwhelmed by the noise response when the noise was at a favorable azimuth, or suppressed by the noise at an unfavorable azimuth. We defined the masked threshold for each unit as the signal-to-noise ratio (SNR) where the signal can just be detected through a change in firing rate. The population masked threshold is the best single-unit threshold for each signal and masker location. Although the individual unit thresholds do not necessarily improve as the signal and masker are spatially separated, the population thresholds do, as do the psychophysical thresholds. Both the absolute values and the shapes of the population threshold curves are similar to those measured psychophysically in humans, suggesting that ITD-sensitive units in the IC may serve as a neural substrate for SRM at low frequencies.

We then developed a model of the responses to SRM stimuli in order to better understand the mechanisms underlying the neural correlate. We started with a standard crosscorrelator model receiving

inputs from a realistic simulation of the auditory periphery. Although this model generally gave good predictions of the noise-alone response as a function of both azimuth and level, it tended to underestimate the signal response. Reasoning that the chirp signal has a strong envelope modulation at its 40-Hz fundamental frequency, and that IC neurons are often preferentially sensitive to envelope modulations in that frequency range, we added sensitivity to the rate of envelope modulation to our model. This envelope processing effectively boosts the signal response relative to the noise response because the signal is highly modulated while the noise is not. In general, the new model accurately predicted single-unit responses to both the noise alone and the signal in noise. This new model, which combines mechanisms of binaural processing and sensitivity to the stimulus envelope, gives quantitative predictions of SRM at the level of both human behavior and individual neuron responses.

Our results suggest that the auditory system uses the temporal structure of sounds as well as binaural cues to detect low-frequency signals in noise. These results are significant because most natural sounds, including speech, have pronounced envelope modulations that previous models of binaural detection have not utilized. Ultimately, our quantitative description of the responses of the IC units to signals in noise may lead to improved performance for hearing aids in challenging acoustic environments.

### **3.4 Auditory-nerve Responses to “Transposed Stimuli”**

Although listeners are sensitive to ITD in the envelope of high-frequency sounds, ITD discrimination performance is poorer for high-frequency sinusoidally amplitude-modulated (SAM) tones than for low-frequency pure tones. It has been suggested that ITD sensitivity at high frequencies might be improved by using “transposed stimuli” formed by modulating a high-frequency carrier by a half-wave rectified sinusoid. The rationale for transposed stimuli is to produce the same temporal discharge patterns in high-frequency neurons as observed in low-frequency neurons for pure tone stimuli. Transposed stimuli have also been used to test the ability of listeners to utilize temporal information delivered to high-frequency regions in forming complex pitch percepts. We ran physiological experiments to test whether the responses of AN fibers to transposed stimuli resemble responses to pure tones and how they differ from responses to SAM tones.

We measured responses of high-frequency AN fibers in anesthetized cats to SAM tones and transposed stimuli with modulation frequencies ranging from 60 to 1000 Hz. Phase locking to the modulation frequency was always greater for a transposed stimulus than for a SAM tone having the same carrier and modulation frequencies. However, for both SAM and transposed stimuli, phase locking degraded with increasing stimulus level once it exceeded a few dB above threshold. This result contrasts with responses to pure tones where the phase locking remains stable at moderate and high sound levels.

Our finding that temporal discharge patterns of AN fibers to transposed stimuli better resemble responses to pure tones than do responses to SAM tones is consistent with the rationale for using transposed stimuli in studies of pitch and binaural hearing. However, responses to transposed stimuli clearly differ from responses to pure tones in their level dependence, suggesting that the level dependence of psychophysical performance with transposed stimuli should be systematically examined in further studies.

### **3.5 Responses of Local Neural Populations in the Inferior Colliculus**

Electrophysiological and anatomical studies have revealed a clear tonotopic organization in the central nucleus of the IC. Studies of connection anatomy further suggest that many brainstem nuclei project to the IC in a focused manner, creating local regions of common input. These observations suggest that neighboring neurons receive similar inputs, and may therefore exhibit similar response properties.

To test this hypothesis, we used ‘tetrodes’, four channel electrodes spaced about 25 $\mu$ m apart, to simultaneously record from 2-6 single-units in the IC of anesthetized cats. We find that, while such neighboring units usually have similar best frequencies (BF) and thresholds, their other response properties can differ sharply. Among 37 pairs of units for which frequency response areas were measured at ~20 dB above threshold, 49% had half bandwidths differing by more than 50%, and some differed by as much as a factor of 10. Among 57 pairs for which temporal response patterns to tone-

bursts were measured, only 23% had similar patterns. Usually, units with very wide bandwidths had Onset temporal discharge patterns. Consistent with this heterogeneity, we found no evidence for cross-correlation between discharge patterns of neighboring units.

These results suggest that, despite the clear tonotopic arrangement of the IC, neighboring cells with similar BFs do not necessarily display similar response properties. Two likely causes for this heterogeneity are differences in intrinsic membrane properties and in distributions and types of synaptic inputs. Since responses of IC neurons seem to arise from inputs spanning a wide range of BFs, some of the differences we see in the frequency response areas of neighboring neurons may result from differences in the strength of inputs that determine off-BF behavior. The differences in temporal discharge patterns may be due in part to differences in intrinsic membrane properties, particularly in the types and distribution of K<sup>+</sup> channels.

## Publications

### Journal Articles Published

S. Kalluri and B. Delgutte, "Mathematical Models of Cochlear Nucleus Onset Neurons. I. Point Neuron with Many Weak Synaptic Inputs," *J. Comput. Neurosci.* 14: 71-90 (2003a).

S. Kalluri and B. Delgutte, "Mathematical Models of Cochlear Nucleus Onset Neurons. II. Model with Dynamic Spike-blocking State," *J. Comput. Neurosci.* 14: 91-110 (2003b).

L.M. Litvak, Z.M. Smith, B. Delgutte, and D.K. Eddington, "Desynchronization of Electrically-evoked Auditory-nerve Activity by High-frequency Pulse Trains of Long Duration," *J. Acoust. Soc. Am.* 114: 2066-2078 (2003a).

L.M. Litvak, B. Delgutte, and D.K. Eddington, "Improved Temporal Coding of Sinusoids in Electric Stimulation of the Auditory Nerve Using Desynchronizing Pulse Trains," *J. Acoust. Soc. Am.* 114: 2079-2098 (2003b).

L.M. Litvak, B. Delgutte, and D.K. Eddington, "Improved Neural Representation of Vowels in Electric Stimulation Using Desynchronizing Pulse Trains," *J. Acoust. Soc. Am.* 114:2099-2111 (2003c).

### Journal Articles Submitted for Publication

K.E. Hancock and B. Delgutte, "A Physiologically Based Model of Interaural Time Difference Discrimination," submitted to *J. Neurosci.*

### Book Chapters

L. Cedolin and B. Delgutte, "Representations of the Pitch of Complex Tones in the Auditory Nerve," in *Auditory Signal Processing: Physiology, Psychoacoustics, and Models*, eds. D. Pressnitzer, A. de Cheveigne, S. McAdams and L. Collet (Springer, in press).

C.C. Lane, N. Kopco, B. Delgutte, B.G. Shinn-Cunningham, and H.S. Colburn, "A Cat's Cocktail Party: Psychophysical, Neurophysiological, and Computational Studies of Spatial Release from Masking," in: *Auditory Signal Processing: Physiology, Psychoacoustics, and Models*, eds. D. Pressnitzer, A. de Cheveigne, S. McAdams and L. Collet (Springer, in press).

**Abstracts**

L. Cedolin and B. Delgutte, "Dual Representation of the Pitch of Complex Tones in the Auditory Nerve," *Abstr. Assoc. Res. Otolaryngol.* 26:46 (2003).

K.E. Hancock and B. Delgutte, "Tuning to Interaural Time Difference in the Cat Inferior Colliculus: Dependence on Characteristic Frequency," *Abstr. Assoc. Res. Otolaryngol.* 26:179 (2003).

C.C. Lane, B. Delgutte, and H.S. Colburn, "A Population of ITD Sensitive Units in the Cat Inferior Colliculus Shows Correlates of Spatial Release from Masking," *Abstr. Assoc. Res. Otolaryngol.* 26:179 (2003).

C.C. Lane, B. Delgutte, and H.S. Colburn, "Signal Detection in the Auditory Midbrain: Neural Correlates and Mechanisms of Spatial Release from Masking," *Abstr. Assoc. Res. Otolaryngol.* 27 (2004).

C.V. Seshagiri and B. Delgutte, "Simultaneous Single-unit Recording from Local Populations in the Inferior Colliculus," *Abstr. Assoc. Res. Otolaryngol.* 26:174 (2003).

C.V. Seshagiri and B. Delgutte, "Responses of Local Neural Populations in the Inferior Colliculus," *Abstr. Assoc. Res. Otolaryngol.* 27 (2004).

Z.M. Smith and B. Delgutte, "Binaural Interactions with Bilateral Electric Stimulation of the Cochlea: Evoked Potential and Single-unit Measures," *Abstr. Assoc. Res. Otolaryngol.* 26:198 (2003).

**Thesis**

C.C. Lane, *Neural Correlates and Mechanisms of Spatial Release from Masking in the Auditory Midbrain*, Doctoral Dissertation, Harvard-MIT Division of Health Sciences and Technology, MIT, 2003.

#### **4. Bilateral Cochlear Implants: Physiological and Psychophysical Studies**

##### **Sponsor:**

National Institutes of Health – National Institute on Deafness and Communication Disorders  
Grant DC05775

##### **Project Staff**

Dr. Bertrand Delgutte, Dr. Donald K. Eddington, Dr. H. Steven Colburn, Zachary M Smith, Becky B. Poon, Hui Nam

The long-term goal of our research is to identify the best stimulus configurations for effectively delivering binaural information with bilateral cochlear implants using closely-integrated neurophysiological, psychophysical, and computational studies. Studies in the past year have focused on measuring the basic sensitivity to interaural time differences (ITD) of bilaterally implanted human subjects and neurons in the auditory midbrain of implanted cats.

##### **4.1 Neural Coding of ITD in the Inferior Colliculus for Bilateral Electric Stimulation of the Cochlea**

The neural processing of binaural cues in normal-hearing listeners is essential for accurate sound localization and speech reception in noisy environments. Bilateral cochlear implantation is becoming increasingly common in the hope of restoring the advantages of binaural hearing to cochlear implant users. However, little is known about binaural interactions in auditory neurons with electric stimulation. To find out, we recorded from single-units in the inferior colliculus (IC) of acutely deafened, anesthetized cats in response to electric stimulation delivered through bilaterally-implanted intracochlear electrodes. We focused on the neural coding of interaural timing differences (ITD) for pulse trains with and without sinusoidal amplitude modulation (SAM).

Most cells in the central nucleus of the IC were found to be sensitive to ITD with low-rate (<100 pps) pulsatile stimuli. Single-unit responses to trains of biphasic pulses elicited strongly phase-locked spikes throughout the duration of the stimulus. With increasing current level, ITD tuning broadened and could saturate as little as 2-3 dB above threshold for some units. Best ITD and half-width of ITD tuning fell within the ranges expected with acoustic stimulation. When higher-rate pulse trains were employed (>200 Hz), typically only onset responses were observed.

Responses to SAM pulse trains with a carrier rate of 1 kHz and modulation frequency of 40 Hz were also recorded in some IC neurons. ITDs were introduced independently to the modulation and the carrier. Most neurons showed sensitivity to ITDs in both modulation and carrier.

##### **4.2 ITD Sensitivity of Bilaterally Implanted Human Subjects**

Most of this first year's effort in psychophysics was directed at developing the hardware/software systems necessary to make the proposed measurements. In addition, preliminary measures of just-noticeable differences (JNDs) in ITD were made using single interaural electrode pairs in three bilaterally-implanted subjects. Stimuli were both unmodulated pulse trains and SAM pulse trains. For the SAM pulse trains, ITDs were present only in the envelope, not the carrier. We hypothesized that high-rate SAM trains might produce more natural temporal patterns of discharge in the auditory nerve – and therefore better ITD sensitivity – than unmodulated pulse trains.

For unmodulated 50 pps pulse trains, the ITD JNDs in two subjects were about 200  $\mu$ s, approaching the JNDs for 50-Hz tones in normal-hearing subjects. A third subject had significantly poorer JNDs. However, when the pulse rate was increased to 200 pps, JNDs for the two best subjects increased to 250-300  $\mu$ s, which is much higher than the 40  $\mu$ s JNDs for 200 Hz pure tones in normal-hearing subjects.

In the case of SAM pulse trains, the ITD JNDs for a 200 pps pulse train amplitude-modulated at 50 Hz were very poor, exceeding 1 ms. Performance improved dramatically when the pulse rate was increased to 1000 pps, then showed a small, but significant further improvement at 5000 pps. The JNDs for the

5000 pps SAM pulse train were comparable to those for the 50 pps unmodulated pulse train.

### *Significance*

Several aspects of our psychophysical and physiological results are promising for the goal of successfully transmitting ITD information to cochlear implant users. The near normal ITD JNDs measured for two subjects using either 50 pps unmodulated pulse trains or 50-Hz SAM pulse trains demonstrate a retention of ITD sensitivity in spite of suffering from bilateral profound sensorineural hearing impairment for more than two years. Correspondingly, electric ITD tuning to low-rate pulse trains in most IC cells is as sharp as that seen in acoustic responses.

These similarities in ITD processing between normal hearing and implanted subjects appear to hold over only a limited set of conditions. In the neural data, sharp ITD tuning is restricted to a very small dynamic range. In psychophysics, the good ITD discrimination with 50-pps pulse trains degrades when the pulse rate is increased to 200 pps. This finding is consistent with our observation that the responses of most IC neurons become limited to stimulus onset as the pulse rate is increased over 100 pps, resulting in a less precise encoding of ITD.

The improvement in ITD discrimination performance with increasing pulse rate for SAM trains is broadly consistent with our hypothesis that such stimuli may produce more natural temporal pattern of discharge in the auditory nerve, thereby aiding ITD processing. However, this improvement was nonmonotonic, showing a broad plateau near 1000-2000 pps. Our physiological data show that, for these carrier rates, IC neurons are sensitive to ITDs in both the carrier and the envelope, so that the zero carrier ITD in psychophysical experiments may have caused a degradation in performance. Consistent with this interpretation, performance improved when the pulse rate was increased to 5000 pps, above the limit of phase locking in the auditory nerve. Further improvements might be obtained by using stimuli superimposed upon an ongoing desynchronizing pulse train, as originally suggested by Rubinstein and verified by our auditory-nerve experiments.

Overall, our physiological and psychophysical results show that many different stimulus parameters and subject-related factors seem to influence ITD sensitivity with bilateral electric stimulation, suggesting that precise adjustments in processing strategies will be necessary for effective delivery of binaural cues.

## **Publications**

### **Abstracts**

B.B. Poon, D.K. Eddington and H.S. Colburn, "Sound Localization with Bilateral Cochlear Implants," *Conference on Implantable Auditory Prostheses*, Pacific Grove, CA, p. 87 (2003).

Z.M. Smith and B. Delgutte, "Binaural Interactions with Bilateral Electric Stimulation of the Cochlea: Evoked Potential and Single-unit Measures," *Abstr. Assoc. Res. Otolaryngol.*, 26 (2003).

Z.M. Smith and B. Delgutte, "Neural Sensitivity to Interaural Timing Differences with Bilateral Electric Stimulation of the Cochlea," *Conference on Implantable Auditory Prostheses* Pacific Grove, CA, p. 63 (2003).